

Measurement of the W Boson Mass

S. Abachi,¹⁴ B. Abbott,²⁸ M. Abolins,²⁵ B. S. Acharya,⁴³ I. Adam,¹² D. L. Adams,³⁷ M. Adams,¹⁷ S. Ahn,¹⁴ H. Aihara,²² J. Alitti,⁴⁰ G. Álvarez,¹⁸ G. A. Alves,¹⁰ E. Amidi,²⁹ N. Amos,²⁴ E. W. Anderson,¹⁹ S. H. Aronson,⁴ R. Astur,⁴² R. E. Avery,³¹ M. M. Baarmand,⁴² A. Baden,²³ V. Balamurali,³² J. Balderston,¹⁶ B. Baldin,¹⁴ S. Banerjee,⁴³ J. Bantly,⁵ J. F. Bartlett,¹⁴ K. Bazizi,³⁹ A. Belyaev,²⁶ J. Bendich,²² S. B. Beri,³⁴ I. Bertram,³¹ V. A. Bezzubov,³⁵ P. C. Bhat,¹⁴ V. Bhatnagar,³⁴ M. Bhattacharjee,¹³ A. Bischoff,⁹ N. Biswas,³² G. Blazey,¹⁴ S. Blessing,¹⁵ P. Bloom,⁷ A. Boehnlein,¹⁴ N. I. Bojko,³⁵ F. Borchering,¹⁴ J. Borders,³⁹ C. Boswell,⁹ A. Brandt,¹⁴ R. Brock,²⁵ A. Bross,¹⁴ D. Buchholz,³¹ V. S. Burtovoi,³⁵ J. M. Butler,³ W. Carvalho,¹⁰ D. Casey,³⁹ H. Castilla-Valdez,¹¹ D. Chakraborty,⁴² S.-M. Chang,²⁹ S. V. Chekulaev,³⁵ L.-P. Chen,²² W. Chen,⁴² S. Choi,⁴¹ S. Chopra,²⁴ B. C. Choudhary,⁹ J. H. Christenson,¹⁴ M. Chung,¹⁷ D. Claes,⁴² A. R. Clark,²² W. G. Cobau,²³ J. Cochran,⁹ W. E. Cooper,¹⁴ C. Cretsinger,³⁹ D. Cullen-Vidal,⁵ M. A. C. Cummings,¹⁶ D. Cutts,⁵ O. I. Dahl,²² K. De,⁴⁴ M. Demarteau,¹⁴ N. Denisenko,¹⁴ D. Denisov,¹⁴ S. P. Denisov,³⁵ H. T. Diehl,¹⁴ M. Diesburg,¹⁴ G. Di Loreto,²⁵ R. Dixon,¹⁴ P. Draper,⁴⁴ J. Drinkard,⁸ Y. Ducros,⁴⁰ L. V. Dudko,²⁶ S. R. Dugad,⁴³ D. Edmunds,²⁵ J. Ellison,⁹ V. D. Elvira,⁴² R. Engelmann,⁴² S. Eno,²³ G. Eppley,³⁷ P. Ermolov,²⁶ O. V. Eroshin,³⁵ V. N. Evdokimov,³⁵ S. Fahey,²⁵ T. Fahland,⁵ M. Fatyga,⁴ M. K. Fatyga,³⁹ J. Featherly,⁴ S. Feher,¹⁴ D. Fein,² T. Ferbel,³⁹ G. Finocchiaro,⁴² H. E. Fisk,¹⁴ Y. Fisyak,⁷ E. Flattum,²⁵ G. E. Forden,² M. Fortner,³⁰ K. C. Frame,²⁵ P. Franzini,¹² S. Fuess,¹⁴ E. Gallas,⁴⁴ A. N. Galyaev,³⁵ T. L. Geld,²⁵ R. J. Genik II,²⁵ K. Genser,¹⁴ C. E. Gerber,¹⁴ B. Gibbard,⁴ V. Glebov,³⁹ S. Glenn,⁷ J. F. Glicenstein,⁴⁰ B. Gobbi,³¹ M. Goforth,¹⁵ A. Goldschmidt,²² B. Gómez,¹ G. Gomez,²³ P. I. Goncharov,³⁵ J. L. González Solís,¹¹ H. Gordon,⁴ L. T. Goss,⁴⁵ N. Graf,⁴ P. D. Grannis,⁴² D. R. Green,¹⁴ J. Green,³⁰ H. Greenlee,¹⁴ G. Griffin,⁸ N. Grossman,¹⁴ P. Grudberg,²² S. Grünendahl,³⁹ W. X. Gu,^{14,*} G. Guglielmo,³³ J. A. Guida,² J. M. Guida,⁵ W. Guryn,⁴ S. N. Gurzhiev,³⁵ P. Gutierrez,³³ Y. E. Gutnikov,³⁵ N. J. Hadley,²³ H. Haggerty,¹⁴ S. Hagopian,¹⁵ V. Hagopian,¹⁵ K. S. Hahn,³⁹ R. E. Hall,⁸ S. Hansen,¹⁴ R. Hatcher,²⁵ J. M. Hauptman,¹⁹ D. Hedin,³⁰ A. P. Heinson,⁹ U. Heintz,¹⁴ R. Hernández-Montoya,¹¹ T. Heuring,¹⁵ R. Hirosky,¹⁵ J. D. Hobbs,¹⁴ B. Hoeneisen,^{1,†} J. S. Hoftun,⁵ F. Hsieh,²⁴ Tao Hu,¹⁴ Ting Hu,⁴² Tong Hu,¹⁸ T. Huehn,⁹ S. Igarashi,¹⁴ A. S. Ito,¹⁴ E. James,² J. Jaques,³² S. A. Jerger,²⁵ J. Z.-Y. Jiang,⁴² T. Joffe-Minor,³¹ H. Johari,²⁹ K. Johns,² M. Johnson,¹⁴ H. Johnstad,²⁹ A. Jonckheere,¹⁴ M. Jones,¹⁶ H. Jöstlein,¹⁴ S. Y. Jun,³¹ C. K. Jung,⁴² S. Kahn,⁴ G. Kalbfleisch,³³ J. S. Kang,²⁰ R. Kehoe,³² M. L. Kelly,³² L. Kerth,²² C. L. Kim,²⁰ S. K. Kim,⁴¹ A. Klatchko,¹⁵ B. Klima,¹⁴ B. I. Klochkov,³⁵ C. Klopfenstein,⁷ V. I. Klyukhin,³⁵ V. I. Kochetkov,³⁵ J. M. Kohli,³⁴ D. Koltick,³⁶ A. V. Kostritskiy,³⁵ J. Kotcher,⁴ J. Kourlas,²⁸ A. V. Kozelov,³⁵ E. A. Kozlovski,³⁵ J. Krane,²⁷ M. R. Krishnaswamy,⁴³ S. Krzywdzinski,¹⁴ S. Kunori,²³ S. Lami,⁴² G. Landsberg,¹⁴ B. Lauer,¹⁹ J.-F. Lebrat,⁴⁰ A. Leflat,²⁶ H. Li,⁴² J. Li,⁴⁴ Y. K. Li,³¹ Q. Z. Li-Demarteau,¹⁴ J. G. R. Lima,³⁸ D. Lincoln,²⁴ S. L. Linn,¹⁵ J. Linnemann,²⁵ R. Lipton,¹⁴ Y. C. Liu,³¹ F. Lobkowicz,³⁹ S. C. Loken,²² S. Lökös,⁴² L. Lueking,¹⁴ A. L. Lyon,²³ A. K. A. Maciel,¹⁰ R. J. Madaras,²² R. Madden,¹⁵ L. Magaña-Mendoza,¹¹ S. Mani,⁷ H. S. Mao,¹⁴ R. Markeloff,³⁰ L. Markosky,² T. Marshall,¹⁸ M. I. Martin,¹⁴ B. May,³¹ A. A. Mayorov,³⁵ R. McCarthy,⁴² T. McKibben,¹⁷ J. McKinley,²⁵ T. McMahon,³³ H. L. Melanson,¹⁴ J. R. T. de Mello Neto,³⁸ K. W. Merritt,¹⁴ H. Miettinen,³⁷ A. Mincer,²⁸ J. M. de Miranda,¹⁰ C. S. Mishra,¹⁴ N. Mokhov,¹⁴ N. K. Mondal,⁴³ H. E. Montgomery,¹⁴ P. Mooney,¹ H. da Motta,¹⁰ M. Mudan,²⁸ C. Murphy,¹⁷ F. Nang,⁵ M. Narain,¹⁴ V. S. Narasimham,⁴³ A. Narayanan,² H. A. Neal,²⁴ J. P. Negret,¹ E. Neis,²⁴ P. Nemethy,²⁸ D. Nešić,⁵ M. Nicola,¹⁰ D. Norman,⁴⁵ L. Oesch,²⁴ V. Oguri,³⁸ E. Oltman,²² N. Oshima,¹⁴ D. Owen,²⁵ P. Padley,³⁷ M. Pang,¹⁹ A. Para,¹⁴ C. H. Park,¹⁴ Y. M. Park,²¹ R. Partridge,⁵ N. Parua,⁴³ M. Paterno,³⁹ J. Perkins,⁴⁴ A. Peryshkin,¹⁴ M. Peters,¹⁶ H. Piekarczyk,¹⁵ Y. Pischalnikov,³⁶ V. M. Podstavkov,³⁵ B. G. Pope,²⁵ H. B. Prosper,¹⁵ S. Protopopescu,⁴ D. Pušeljčić,²² J. Qian,²⁴ P. Z. Quintas,¹⁴ R. Raja,¹⁴ S. Rajagopalan,⁴² O. Ramirez,¹⁷ M. V. S. Rao,⁴³ P. A. Rapidis,¹⁴ L. Rasmussen,⁴² S. Reucroft,²⁹ M. Rijssenbeek,⁴² T. Rockwell,²⁵ N. A. Roe,²² P. Rubinov,³¹ R. Ruchti,³² J. Rutherford,² A. Sánchez-Hernández,¹¹ A. Santoro,¹⁰ L. Sawyer,⁴⁴ R. D. Schamberger,⁴² H. Schellman,³¹ J. Sculli,²⁸ E. Shabalina,²⁶ C. Shaffer,¹⁵ H. C. Shankar,⁴³ R. K. Shivpuri,¹³ M. Shupe,² J. B. Singh,³⁴ V. Sirotenko,³⁰ W. Smart,¹⁴ A. Smith,² R. P. Smith,¹⁴ R. Snihur,³¹ G. R. Snow,²⁷ J. Snow,³³ S. Snyder,⁴ J. Solomon,¹⁷ P. M. Sood,³⁴ M. Sosebee,⁴⁴ N. Sotnikova,²⁶ M. Souza,¹⁰ A. L. Spadafora,²² R. W. Stephens,⁴⁴ M. L. Stevenson,²² D. Stewart,²⁴ D. A. Stoianova,³⁵ D. Stoker,⁸ K. Streets,²⁸ M. Strovink,²² A. Sznajder,¹⁰ P. Tamburello,²³ J. Tarazi,⁸ M. Tartaglia,¹⁴ T. L. Taylor,³¹ J. Thompson,²³ T. G. Trippe,²² P. M. Tuts,¹² N. Varelas,²⁵ E. W. Varnes,²² P. R. G. Virador,²² D. Vititoe,² A. A. Volkov,³⁵ A. P. Vorobiev,³⁵ H. D. Wahl,¹⁵ G. Wang,¹⁵ J. Warchol,³² G. Watts,⁵ M. Wayne,³² H. Weerts,²⁵ A. White,⁴⁴

J. T. White,⁴⁵ J. A. Wightman,¹⁹ J. Wilcox,²⁹ S. Willis,³⁰ S. J. Wimpenny,⁹ J. V. D. Wirjawan,⁴⁵ J. Womersley,¹⁴
 E. Won,³⁹ D. R. Wood,²⁹ H. Xu,⁵ R. Yamada,¹⁴ P. Yamin,⁴ C. Yanagisawa,⁴² J. Yang,²⁸ T. Yasuda,²⁹ P. Yepes,³⁷
 C. Yoshikawa,¹⁶ S. Youssef,¹⁵ J. Yu,¹⁴ Y. Yu,⁴¹ Q. Zhu,²⁸ Z. H. Zhu,³⁹ D. Zieminska,¹⁸ A. Zieminski,¹⁸
 E. G. Zverev,²⁶ and A. Zylberstejn,⁴⁰

(D0 Collaboration)

- ¹Universidad de los Andes, Bogotá, Colombia
²University of Arizona, Tucson, Arizona 85721
³Boston University, Boston, Massachusetts 02215
⁴Brookhaven National Laboratory, Upton, New York 11973
⁵Brown University, Providence, Rhode Island 02912
⁶Universidad de Buenos Aires, Buenos Aires, Argentina
⁷University of California, Davis, California 95616
⁸University of California, Irvine, California 92717
⁹University of California, Riverside, California 92521
¹⁰LAFEX, Centro Brasileiro de Pesquisas Físicas, Rio de Janeiro, Brazil
¹¹Centro de Investigación y de Estudios Avanzados, Mexico City, Mexico
¹²Columbia University, New York, New York 10027
¹³Delhi University, Delhi, India 110007
¹⁴Fermi National Accelerator Laboratory, Batavia, Illinois 60510
¹⁵Florida State University, Tallahassee, Florida 32306
¹⁶University of Hawaii, Honolulu, Hawaii 96822
¹⁷University of Illinois at Chicago, Chicago, Illinois 60607
¹⁸Indiana University, Bloomington, Indiana 47405
¹⁹Iowa State University, Ames, Iowa 50011
²⁰Korea University, Seoul, Korea
²¹Kyungsung University, Pusan, Korea
²²Lawrence Berkeley National Laboratory and University of California, Berkeley, California 94720
²³University of Maryland, College Park, Maryland 20742
²⁴University of Michigan, Ann Arbor, Michigan 48109
²⁵Michigan State University, East Lansing, Michigan 48824
²⁶Moscow State University, Moscow, Russia
²⁷University of Nebraska, Lincoln, Nebraska 68588
²⁸New York University, New York, New York 10003
²⁹Northeastern University, Boston, Massachusetts 02115
³⁰Northern Illinois University, DeKalb, Illinois 60115
³¹Northwestern University, Evanston, Illinois 60208
³²University of Notre Dame, Notre Dame, Indiana 46556
³³University of Oklahoma, Norman, Oklahoma 73019
³⁴University of Panjab, Chandigarh 16-00-14, India
³⁵Institute for High Energy Physics, 142-284 Protvino, Russia
³⁶Purdue University, West Lafayette, Indiana 47907
³⁷Rice University, Houston, Texas 77251
³⁸Universidade Estadual do Rio de Janeiro, Rio de Janeiro, Brazil
³⁹University of Rochester, Rochester, New York 14627
⁴⁰Commissariat a L'Énergie Atomique, Departement d'Astrophysique, Physique des Particules, Physique Nucleaire et
 d'Instrumentation Associee/Service de Physique des Particules, CE-Saclay, France
⁴¹Seoul National University, Seoul, Korea
⁴²State University of New York, Stony Brook, New York 11794
⁴³Tata Institute of Fundamental Research, Colaba, Bombay 400005, India
⁴⁴University of Texas, Arlington, Texas 76019
⁴⁵Texas A&M University, College Station, Texas 77843

(Received 11 July 1996)

A measurement of the mass of the W boson is presented based on a sample of 5982 $W \rightarrow e\nu$ decays observed in $p\bar{p}$ collisions at $\sqrt{s} = 1.8$ TeV with the D0 detector during the 1992–1993 run. From a fit to the transverse mass spectrum, combined with measurements of the Z boson mass, the W boson mass is measured to be $M_W = 80.350 \pm 0.140(\text{stat}) \pm 0.165(\text{syst}) \pm 0.160(\text{scale})$ GeV $/c^2$. [S0031-9007(96)01446-9]

PACS numbers: 14.70.Fm, 12.15.Ji, 13.38.Be, 13.85.Qk

The parameters of the gauge sector of the electroweak standard model [1] can be taken to be the fine structure constant, the Fermi constant, and the mass of the Z boson, M_Z , all measured to a precision better than 0.01%. Higher order calculations then relate the mass of the W boson, M_W , and the weak mixing angle, θ_W , to these three parameters, the heavy fermion masses, and the Higgs boson mass. Within the standard model, a direct measurement of M_W thus constrains the allowed region for the top quark and Higgs masses. Alternatively, a precision measurement of the W mass, when combined with other measurements of $\sin^2 \theta_W$, provides a test of the standard model. The mass of the W boson has been measured recently in a number of experiments [2]. We present here a new precision measurement.

We have analyzed a sample of $W \rightarrow e\nu$ decays resulting from $p\bar{p}$ collisions at $\sqrt{s} = 1.8$ TeV. This sample, which corresponds to an exposure of ≈ 12.8 pb $^{-1}$, was collected with the D0 detector during the 1992–1993 run at the Fermilab Tevatron collider. Two components of the detector [3] are most relevant to this analysis. The central tracking system is used to reconstruct charged particle tracks and the interaction vertex. A central and two end uranium liquid-argon calorimeters measure the energy flow over a pseudorapidity range $|\eta| \leq 4.2$ [4].

Both $W \rightarrow e\nu$ and $Z \rightarrow e^+e^-$ decays are used in the analysis. The electrons from these decays tend to be isolated and of high transverse momentum, p_T . At the trigger level [5], W candidates were required to have an electromagnetic (EM) energy cluster with transverse energy $E_T = E \sin \theta \geq 20$ GeV and to have missing transverse energy $\cancel{E}_T \geq 20$ GeV. Here $\cancel{E}_T = -\sum_i \vec{E}_{T_i}$, with the sum extending over all calorimeter cells. Z candidates were required to have two EM energy clusters, each with $E_T \geq 10$ GeV.

Off-line selection criteria were imposed on the EM energy cluster of each electron candidate. The transverse and longitudinal shower profiles of the cluster were required to be consistent with those expected for an electron [6]. The energy leakage of the cluster into the hadronic compartment of the calorimeter was required to be less than 10%. The isolation criterion of the cluster was satisfied by requiring the total energy within a cone of radius $R = 0.4$ [7], centered on the electron direction, but outside the EM core of the shower ($R = 0.2$), to be less than 15% of the energy in the EM core. A spatial match of the cluster with a central detector track was required. Electrons with a cluster position in the region between the cryostats ($1.2 < |\eta| < 1.5$) or within 10% of the boundary of a calorimeter module in the central region were eliminated from the data sample.

Having found events with well-identified, isolated electrons and for W bosons the required \cancel{E}_T , kinematic constraints were imposed on the data. The E_T 's of each electron in Z events and of the electron and neutrino in W events were required to exceed 25 GeV. The neu-

trino E_T was equated to the \cancel{E}_T . In addition, the transverse momentum of the W boson, p_T^W , had to be less than 30 GeV/ c . These selection criteria yielded 7234 $W \rightarrow e\nu$ events with the electron in the central calorimeter ($|\eta| < 1.2$), 366 $Z \rightarrow ee$ events with both electrons in the central calorimeter, and 281 $Z \rightarrow ee$ events with one electron in the central and one in an end calorimeter ($1.5 < |\eta| < 2.5$).

Since the longitudinal component of the neutrino momentum is not measured, the W invariant mass cannot be reconstructed. Rather, the mass of the W boson is extracted from the distribution in transverse mass, defined as $m_T^2 = 2|\vec{E}_T^e||\vec{E}_T^\nu|(1 - \cos \varphi_{e\nu})$, where $\varphi_{e\nu}$ is the angle between the electron and neutrino transverse momenta. The electron direction is defined using the centroid of the calorimeter cluster and the weighted average of the z positions of the hits on the track. The uncertainty in determining this angle leads to an uncertainty of 50 MeV/ c^2 on M_W . Since the absolute energy scale of the EM calorimeter is not known with the required precision, the ratio of the measured W and Z masses and the world average Z mass [8] were used to determine the W boson mass. The module-to-module calibration of the central EM calorimeter was determined to a precision of 0.5%. The energy resolution of the central EM calorimeter has been parametrized for this analysis as $\sigma/E = 0.015 \oplus 0.13/\sqrt{E_T} \oplus 0.4/E$, with E in GeV. The sampling term of $0.13/\sqrt{E_T}$ was measured in a test beam; the constant term of $0.015^{+0.006}_{-0.015}$ was determined directly from the observed width of the Z resonance. The uncertainty in the EM energy resolution contributes a 70 MeV/ c^2 uncertainty on M_W .

The EM energy scale of the central calorimeter was determined by comparing the masses measured in $\pi^0 \rightarrow \gamma\gamma$, $J/\psi \rightarrow e^+e^-$, and $Z \rightarrow e^+e^-$ decays to their known values [8,9]. If the electron energy measured in the calorimeter and the true energy are related by $E_{\text{meas}} = \alpha E_{\text{true}} + \delta$, the measured and true mass values are, to first order, related by $m_{\text{meas}} = \alpha m_{\text{true}} + \delta f$. The variable f depends on the decay topology and is given by $f = [2(E_1 + E_2)/m_{\text{meas}}] \sin^2 \gamma/2$, where γ is the opening angle between the two decay products and E_1 and E_2 are their measured energies. Figure 1 shows the constraints on the parameters α and δ obtained independently from the π^0 , the J/ψ , and the Z data. When combined, these three constraints limit α and δ to the shaded elliptical region. Test beam measurements allow for a small nonlinear term in the energy response, which affects both α and δ and alters the ratio M_W/M_Z largely through the effect on δ , as shown by the dotted line in Fig. 1.

Using the measured masses for the observed resonances, the energy scale factor determined is $\alpha = 0.9514 \pm 0.0018^{+0.0061}_{-0.0017}$ and the offset is $\delta = -0.158 \pm 0.015^{+0.03}_{-0.21}$ GeV, where the asymmetric errors are due to possible nonlinearities. The measured off-

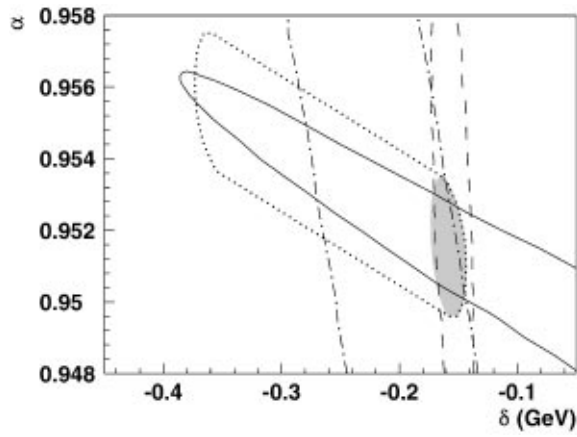


FIG. 1. Constraints on slope α and intercept δ from observed $J/\psi \rightarrow e^+e^-$ (dash-dotted line), $\pi^0 \rightarrow \gamma\gamma$ (dashed line), and $Z \rightarrow e^+e^-$ decays (solid line). The shaded inner contour shows the combined result. The dotted line indicates the allowed area when nonlinear terms, as constrained by test beam measurements, are included.

set is consistent with that determined from test beam data, and has been confirmed by a detailed Monte Carlo study of energy loss in the central detectors. The dependence of the measured ratio of the W mass to Z mass on α and δ may be estimated from

$$\frac{M_W(\alpha, \delta)}{M_Z(\alpha, \delta)} \Big|_{\text{meas}} = \frac{M_W}{M_Z} \Big|_{\text{true}} \times \left[1 + \frac{\delta}{\alpha} \frac{f_W M_Z - f_Z M_W}{M_Z M_W} \right].$$

It should be noted that the W mass is insensitive to α if $\delta = 0$. The uncertainty on the absolute energy scale results in an uncertainty on M_W of $160 \text{ MeV}/c^2$, of which $150 \text{ MeV}/c^2$ is due to the statistics of the Z data sample.

The W mass is obtained from an unbinned maximum-likelihood fit of the data to distributions in m_T , generated as a function of M_W at $100 \text{ MeV}/c^2$ intervals by a fast Monte Carlo simulation. This Monte Carlo models both the production and decay of the vector bosons and the detector response, and relies heavily on experimental data for input. It starts with the double differential W production cross section in p_T and rapidity calculated at next to leading order [10] using the MRSA parton distribution functions (pdf) [11]. The mass of the W boson is generated with a relativistic Breit-Wigner line shape, skewed by the mass dependence of the parton luminosity. In the simulation, the W boson width has been fixed to its measured value, $\Gamma_W = 2.07 \pm 0.06 \text{ GeV}/c^2$ [5]. The uncertainty on Γ_W results in an uncertainty of $20 \text{ MeV}/c^2$ on M_W . The W decay products are then generated in the W rest frame with an angular distribution respecting the polarization of the W . Radiative decays are generated at $\mathcal{O}(\alpha)$ according to [12].

After generation of the kinematics of the event at the four-vector level, the resolutions of the detector are incorporated and the energy scales are set. Minimum bias

(MB) events are used to model the underlying event, mimicking the debris in the event due to spectator parton interactions and the pileup associated with multiple interactions, and including the residual energy from previous beam crossings. The relative response of the hadronic and EM calorimeters is established by studying Z events. To ensure an equivalent event topology between the W and Z events, Z decays in which one electron is in the end calorimeter are included in this study. The transverse momentum balance in Z events is given by $\vec{p}_T^{e_1} + \vec{p}_T^{e_2} + \vec{p}_T^{\text{rec}} + \vec{u}_T = -\vec{E}_T$, where \vec{u}_T is the underlying event contribution and \vec{p}_T^{rec} is the transverse momentum of the recoil to the vector boson. One finds for the average $|\vec{p}_T^{e_1} + \vec{p}_T^{e_2} + \vec{E}_T|^2 = \kappa^2 |\vec{p}_T^{ee}|^2 + |\vec{u}_T|^2$ assuming $|\vec{p}_T^{\text{rec}}| = \kappa |\vec{p}_T^{ee}|$, where \vec{p}_T^{ee} is the transverse momentum of the Z measured from the two electrons. The cross term on the right-hand side averaged to zero since the underlying event vector is randomly distributed with respect to the Z recoil system. Figure 2 shows the distribution of $|\vec{p}_T^{e_1} + \vec{p}_T^{e_2} + \vec{E}_T|^2$ versus $|\vec{p}_T^{ee}|^2$. The data show a linear relation between the EM and hadronic energy scale, and yield $\kappa = 0.83 \pm 0.04$. The intercept yields the magnitude of the underlying event vector, $|\vec{u}_T| = 4.3 \pm 0.3 \text{ GeV}/c$, consistent with the value obtained from MB events. The uncertainty on M_W due to the uncertainty on the hadronic energy scale is $50 \text{ MeV}/c^2$.

The recoil against the vector boson is modeled by a single jet. The transverse momentum of the W is scaled by κ and smeared using a resolution of $0.80/\sqrt{p_T^W} \text{ (GeV)}$, as obtained from our dijet events. The uncertainty on the jet resolution gives a $65 \text{ MeV}/c^2$ uncertainty on M_W . The event is superimposed onto MB events, which simulates the underlying event. The luminosity profile of these MB events is chosen such that the mean number of interactions per crossing is the same as for the W data.

The modeling of the recoil and underlying event are verified and constrained by comparing the p_T of the Z obtained from the two electrons, \vec{p}_T^{ee} , to that obtained from the rest of the event: $-\vec{p}_T^{\text{rec}} - \vec{u}_T$. To minimize

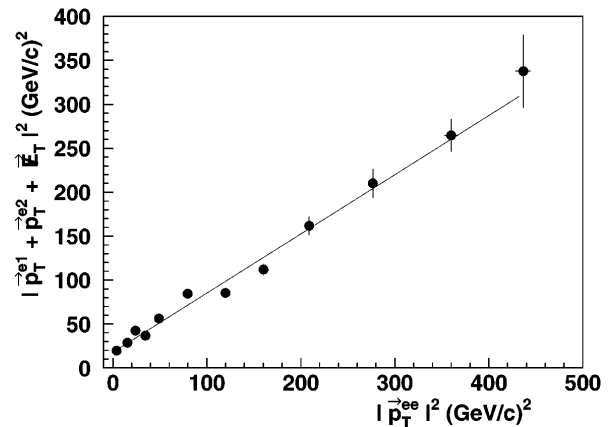


FIG. 2. Distribution of $|\vec{p}_T^{e_1} + \vec{p}_T^{e_2} + \vec{E}_T|^2$ versus $|\vec{p}_T^{ee}|^2$ for Z events

the contribution from the electron energy resolution, the vector sum of these two quantities is projected along the bisector of the two electron directions. Since \vec{u}_T is randomly oriented and has a magnitude $\sim p_T^Z$, the width of the distribution is sensitive to the underlying event contribution, while the mean is largely unaffected. The *rms* of the distribution is 4.44 ± 0.18 GeV/ c . The sensitivity of the width of this distribution to the mean number of MB events that mimic the underlying event is determined by varying the number of MB events in the Monte Carlo. The number of MB events preferred by the data is 0.98 ± 0.06 , consistent with 1. The uncertainty on M_W from the underlying event model is 60 MeV/ c^2 .

The energy underlying the electron was obtained from W events by measuring the energy deposited in a region of the calorimeter the same size as the electron cluster but rotated away from the electron in azimuth. On average, the underlying event adds 205 ± 55 MeV to the energy of central electrons and results in an uncertainty on M_W of 35 MeV/ c^2 .

Detector and reconstruction biases were also modeled in the Monte Carlo simulation. In radiative decays, $W \rightarrow e\nu\gamma$, the $e\nu$ mass does not reconstruct to the W mass unless the photon is clustered with the electron. Also, radiative decays in which the photon is radiated near, but not fully within, the electron cluster can distort the cluster shape causing the electron to fail the shower shape cuts. The same considerations apply to radiative Z decays, and these effects do not cancel completely in the ratio of the masses. Similarly, the recoil system may affect the electron identification, especially if it is close to the electron. A measure of the event selection biases, due to electron shape and isolation cuts, is obtained by studying the projection of the momentum recoiling against the W along the electron p_T direction: $u_{\parallel} \equiv (\vec{p}_T^{\text{rec}} + \vec{u}_T) \cdot \hat{p}_T^e$. An inefficiency in u_{\parallel} would cause a kinematic bias for the W decay products. The efficiency as a function of u_{\parallel} has been determined from the W data using the energy in a cone around the electron, which is used to select isolated electrons. The efficiency was verified using Z decays. For u_{\parallel} values of 20 GeV there is an inefficiency of approximately 10%. The error on M_W resulting from the uncertainty in the u_{\parallel} efficiency is 20 MeV/ c^2 .

The QCD jet background in the W sample was determined from an independent jet data sample to be $(1.6 \pm 0.8)\%$. Inclusion of this background shifts the mass by $+33$ MeV/ c^2 . The background from $Z \rightarrow e^+e^-$ events in which one electron is not identified has been estimated, using ISAJET [13], to be $(0.43 \pm 0.05)\%$. Its effect on M_W is negligible. The uncertainty in the amount of background, and its distribution in transverse mass, gives an uncertainty on M_W of 35 MeV/ c^2 . The 1.3% irreducible background due to $W \rightarrow \tau\nu \rightarrow e\nu\nu\nu$ was included in the Monte Carlo simulation. All other sources of background are negligible.

The distribution in m_T and the Monte Carlo line shape corresponding to the best fit are shown in Fig. 3.

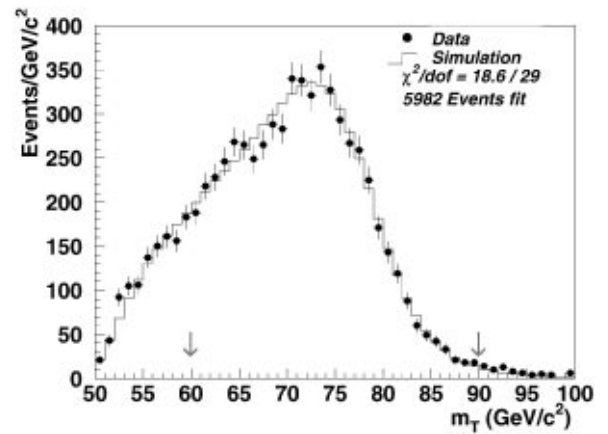


FIG. 3. Best fit to the transverse mass distribution. The arrows indicate the fitting range from which the W mass is extracted.

The mass, extracted from a fit of the 5982 events in the range $60 \leq m_T \leq 90$ GeV/ c^2 , is $M_W = 80.350 \pm 0.140(\text{stat}) \pm 0.165(\text{syst}) \pm 0.160(\text{scale})$ GeV/ c^2 . Table I lists the uncertainties in the measurement, which used the MRSA pdf. As a consistency check, a fit to the p_T^e distribution in the range $30 \leq p_T^e \leq 45$ GeV/ c^2 was performed to extract the W mass. This fit results in a mass 50 MeV/ c^2 lower than when measured from the m_T distribution. The statistical error on this fit is 190 MeV/ c^2 .

The largest systematic uncertainty, beyond those mentioned above, is due to the modeling of the p_T^W spectrum and the pdf's. The correlation between the pdf's and the p_T^W distribution has been addressed. To study the

TABLE I. Uncertainties in the W boson mass measurement.

| Uncertainty | (MeV/ c^2) |
|---------------------------------------|---------------|
| Statistical | 140 |
| Energy scale | 160 |
| Statistical | 150 |
| Z systematics | 35 |
| Calorimeter low energy nonlinearities | 25 |
| Other systematics | 165 |
| Electron energy resolution | 70 |
| Jet energy resolution | 65 |
| pdf's, p_T^W spectrum | 65 |
| Underlying event model | 60 |
| Relative hadronic and EM energy scale | 50 |
| Electron angle calibration | 50 |
| Energy underlying electron | 35 |
| Backgrounds | 35 |
| Radiative decays | 20 |
| u_{\parallel} efficiency | 20 |
| Trigger efficiency | 20 |
| W width | 20 |
| Fitting error | 5 |
| Total | 270 |

uncertainty, parametrizations of the CTEQ3M pdf were obtained [14] incorporating all available data and with the W charge asymmetry [15] data points moved coherently by \pm standard deviation, resulting in a maximum allowed range of pdf's. The parameters governing the nonperturbative part of the p_T^W spectrum [16] were varied simultaneously, as constrained by our measured p_T^Z spectrum. The resulting variation in the spectrum leads to an uncertainty of $65 \text{ MeV}/c^2$ on M_W .

In conclusion, a new measurement of the W mass from a fit to the transverse mass spectrum of $W \rightarrow e\nu$ decays has been presented. The W mass is measured to be $M_W = 80.350 \pm 0.270 \text{ GeV}/c^2$, where all errors have been added in quadrature.

We thank the staffs at Fermilab and the collaborating institutions for their contributions to the success of this work, and acknowledge support from the Department of Energy and National Science Foundation, Commissariat à l'Énergie Atomique (France), Ministries for Atomic Energy and Science and Technology Policy (Russia), CNPq (Brazil), Departments of Atomic Energy and Science and Education (India), Colciencias (Colombia), CONACyT (Mexico), Ministry of Education and KOSEF (Korea), CONICET and UBACyT (Argentina), and the A.P. Sloan Foundation.

*Visitor from IHEP, Beijing, China.

†Visitor from Univ. San Francisco de Quito, Ecuador.

- [1] S. Weinberg, Phys. Rev. Lett. **19**, 1264 (1967); S.L. Glashow, Nucl. Phys. **22**, 579 (1968); A. Salam, in *Elementary Particle Theory*, edited by N. Svartholm (Almqvist and Wiksell, Sweden, 1968), p. 367; S.L. Glashow, J. Illiopoulos, and L. Maiani, Phys. Rev. D **2**, 1285 (1970); M. Kobayashi and M. Maskawa, Prog. Theor. Phys. **49**, 652 (1973).
- [2] UA2 Collaboration, J. Alitti *et al.*, Phys. Lett. B **276**, 354 (1992); CDF Collaboration, F. Abe *et al.*, Phys. Rev. Lett. **65**, 2243 (1990); Phys. Rev. D **43**, 2070 (1991); CDF Collaboration, F. Abe *et al.*, Phys. Rev. Lett. **75**, 11 (1995); F. Abe *et al.*, Phys. Rev. D **52**, 4784 (1995).
- [3] D0 Collaboration, S. Abachi *et al.*, Nucl. Instrum. Methods Phys. Res., Sect. A **338**, 185 (1994).
- [4] Pseudorapidity is defined as $\eta = -\ln \tan(\theta/2)$ where θ is the polar angle with respect to the proton beam.
- [5] D0 Collaboration, S. Abachi *et al.*, Phys. Rev. Lett. **75**, 1456 (1995).
- [6] For more details, see D0 Collaboration, S. Abachi *et al.*, Phys. Rev. D **52**, 4877 (1995).
- [7] R is defined as $R = \sqrt{\Delta\eta^2 + \Delta\varphi^2}$ where $\Delta\eta$ and $\Delta\varphi$ are calculated from the center of the calorimeter cells with respect to the (η, φ) position of the electromagnetic shower.
- [8] We used $M_Z^{\text{LEP}} = 91.1884 \pm 0.0022 \text{ GeV}/c^2$, from P. Renton, contribution to the Lepton-Photon Conference, Beijing, P.R. China, 1995 [Report No. OUNP-95-20].
- [9] The reference mass values used are $M_{J/\psi} = 3.09688 \pm 0.00004 \text{ GeV}/c^2$ and $M_{\pi^0} = 0.1350 \pm 0.0006 \text{ GeV}/c^2$, Particle Data Group, L. Montanet *et al.*, Phys. Rev. D **50**, 1173 (1994).
- [10] G. Ladinsky and C.-P. Yuan, Phys. Rev. D **50**, 4239 (1994).
- [11] A. D. Martin, R. G. Roberts, and W. J. Stirling, Phys. Rev. D **50**, 6734 (1994); **51**, 4756 (1995).
- [12] F. A. Berends and R. Kleiss, Z. Phys. C **27**, 365 (1985).
- [13] F. Paige and S. Protopopescu, BNL Report No. BNL38034, 1986 (unpublished), release 6.49.
- [14] H. L. Lai *et al.*, Phys. Rev. D **51**, 4763 (1995).
- [15] CDF Collaboration, F. Abe *et al.*, Phys. Rev. Lett. **74**, 850 (1995).
- [16] The parametrization of the p_T^W spectrum is most sensitive to variations of the parameter g_2 in the nonperturbative function (see [10]). The range for g_2 as limited by our Z data was $\tilde{g}_2 - 2\sigma < g_2 < \tilde{g}_2 + 4\sigma$ where $\tilde{g}_2 = 0.58_{-0.20}^{+0.10} (\text{GeV}/\hbar c)^2$.